Electronic Supplementary Material (ESI) for New Journal of Chemistry.

Supporting Information

Facile and scalable synthesis of 2D porous Ni/C via a salt-template assisted approach for enhanced urea oxidation reaction and energy-saving hydrogen production

Fengjiao Li[a,b,*], Xiaoming Zhang[a], Shuting Liang[c,*], Mingjuan Sun[a], Xiaolin Zhao[a], Haiwei Chen[a,*], Yanhui Cui[a]

[a] Shenzhen Automotive Research Institute, Beijing Institute of Technology, Shenzhen 518118, Guangdong, China.

[b] National Engineering Laboratory for Electric Vehicles, Beijing Institute of Technology, Beijing 100081, Beijing, China.

[c] Chongqing Key Laboratory of Environmental Materials & Remediation Technologies, Chongqing University of Arts and Sciences, Chongqing 402160, China.

Corresponding author:

Email: lifengjiao@szari.ac.cn; 20180046@cqwu.edu.cn; chenhaiwei@szari.ac.cn.

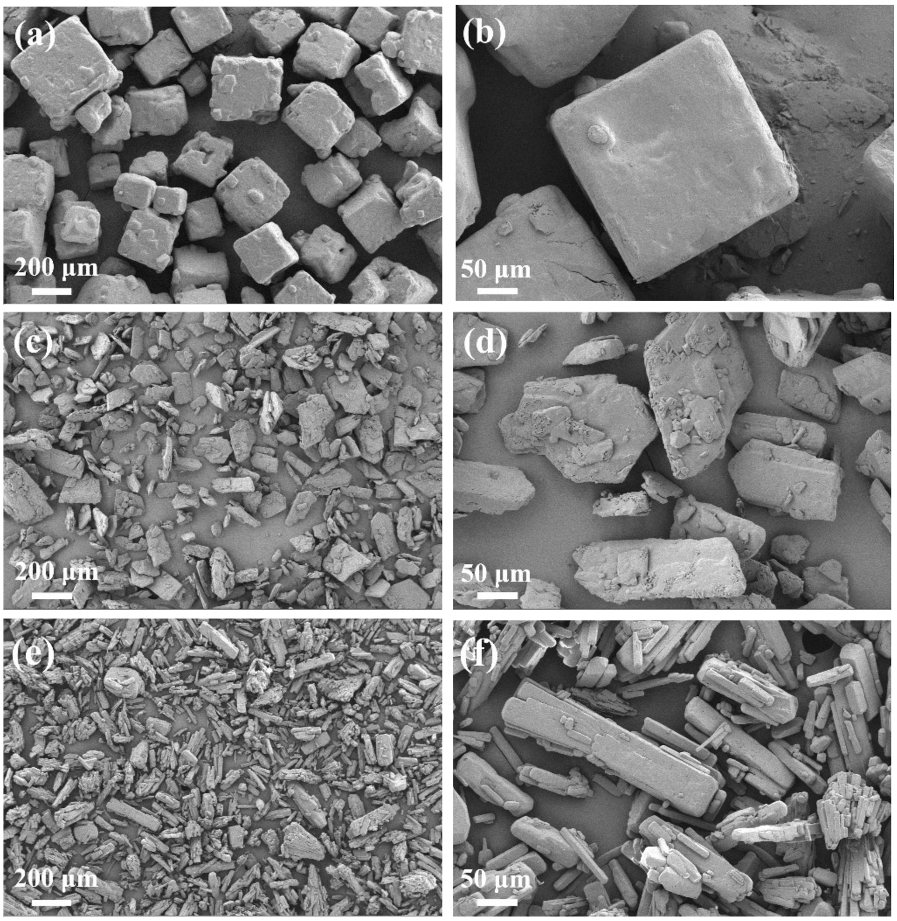

Fig. S1 SEM images of commercial NaCl (a-b), glucose (c-d), and $Ni(Ac)_2{\cdot}4H_2O$ (e-f) crystals at different magnitudes.

The commercial NaCl crystals showed typical cubic morphology with smooth surfaces (**Fig. S1a-b**). The commercial glucose was consisted of faceted tabular crystals (**Fig. S1c-d**). And the commercial $Ni(Ac)_2{\cdot}4H_2O$ was composed of oblong rectangular crystallites (**Fig. S1e-f**).

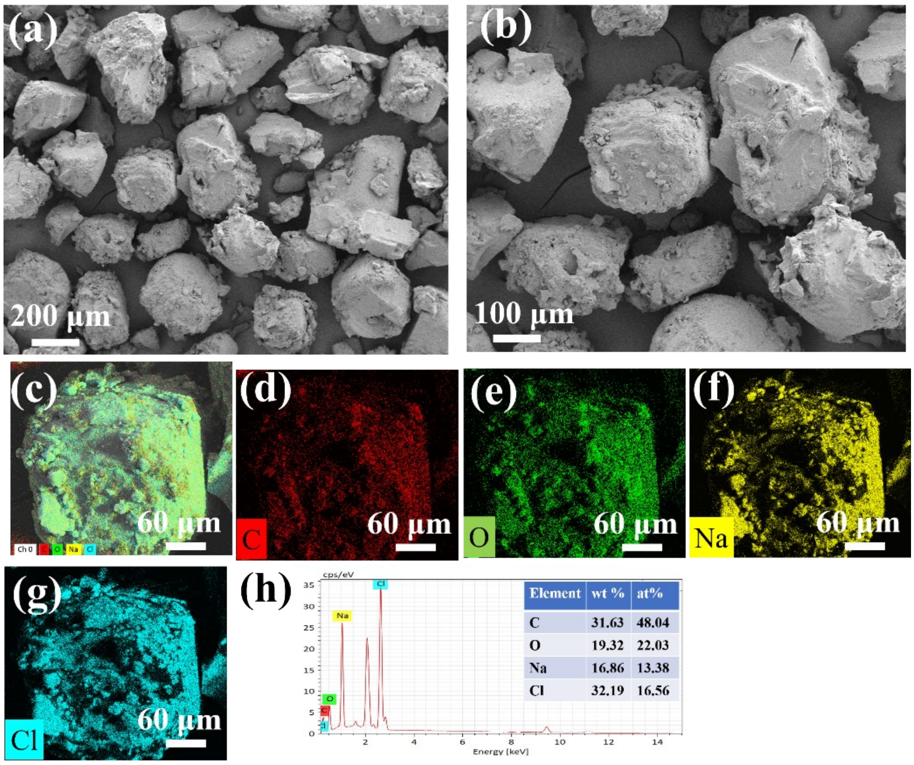

Fig. S2 SEM images (a-b) and element mapping of (c) mix, (d) C, (e) O, (f) Na, (g) Cl and (h) SEM-EDS spectrum of the dried mixture precursor of 0-Ni/CS.

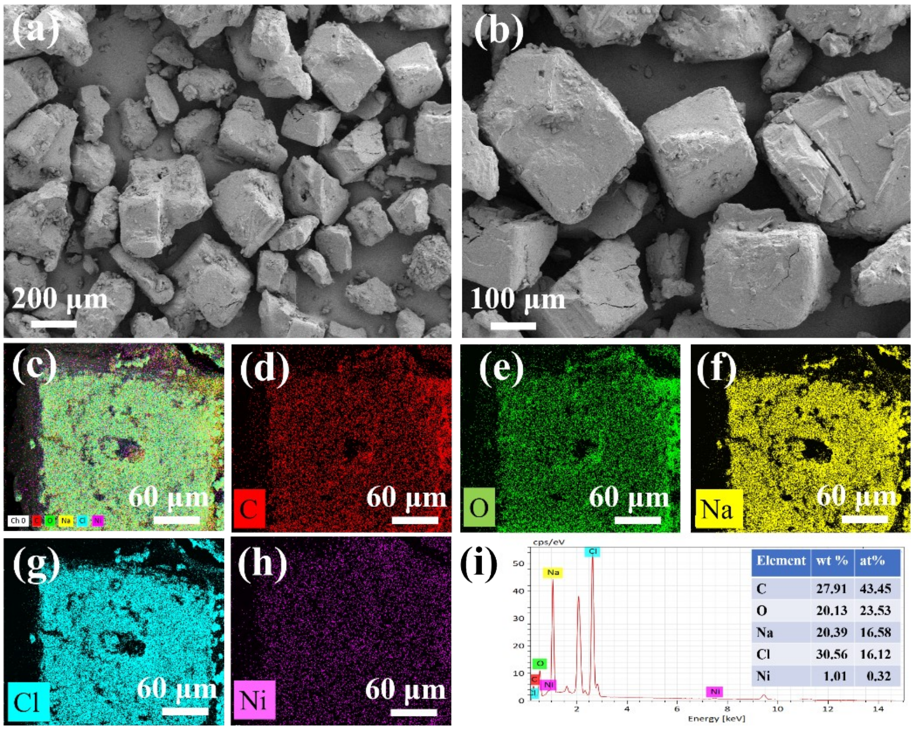

Fig. S3 SEM images (a-b) and element mapping of (c) mix, (d) C, (e) O, (f) Na, (g) Cl, (h) Ni and (i) SEM-EDS spectrum of the dried mixture precursor of 2-Ni/CS.

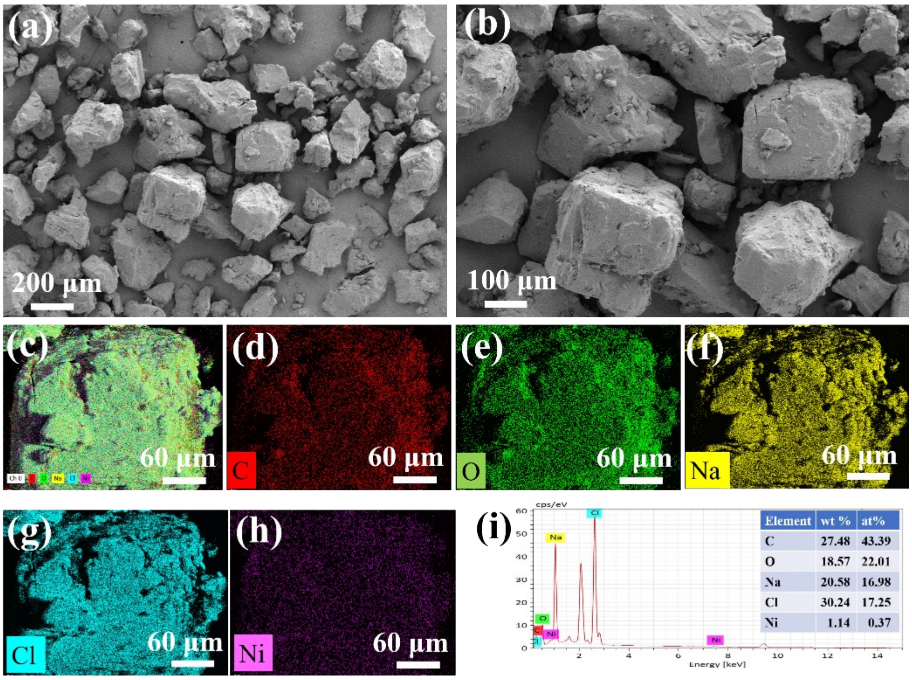

Fig. S4 SEM images (a-b) and element mapping of (c) mix, (d) C, (e) O, (f) Na, (g) Cl, (h) Ni and (i) SEM-EDS spectrum of the dried mixture precursor of 4-Ni/CS.

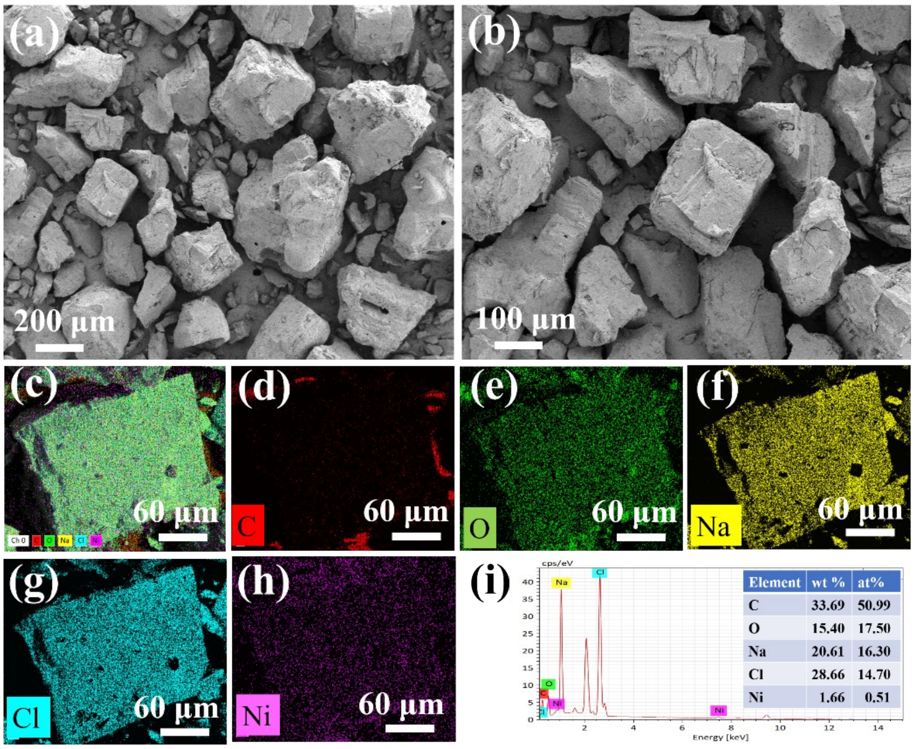

Fig. S5 SEM images (a-b) and element mapping of (c) mix, (d) C, (e) O, (f) Na, (g) Cl, (h) Ni and (i) SEM-EDS spectrum of the dried mixture precursor of 8-Ni/CS.

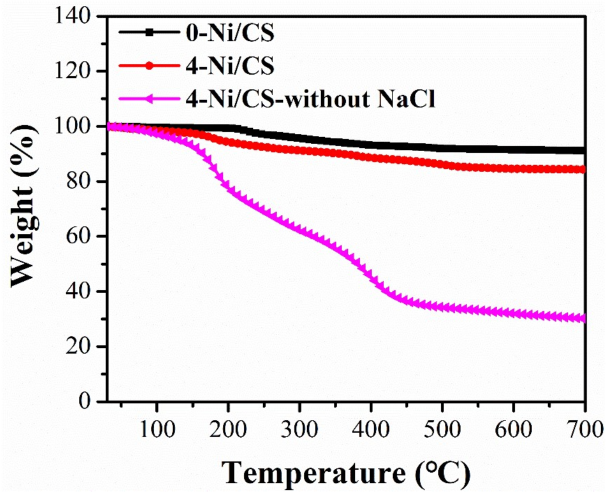

Fig. S6 TG analysis in Ar for the dried 0-Ni/CS, 4-Ni/CS and 4-Ni/CS-without NaCl precursors before carbonization.

Fig. S6 displays the thermal behavior in Ar for the dried 0-Ni/CS, 4-Ni/CS and 4-Ni/CS-without NaCl precursors before carbonization from room temperature to 700 °C with the heating rate of 5 °C min^{-1}. It can be obviously seen that a slight mass loss appeared before 150 °C due to the elimination of moisture. The larger mass loss between 150 °C and 550 °C was mainly attributed to the decomposition of $Ni(Ac)_2·4H_2O$ to form nickel oxide. Afterwards, a very subtle mass loss between 600 and 700 °C was mainly derived from char formation and reduction of nickel oxide to metallic nickel. Notably, 4-Ni/CS without NaCl precursor suffered from a huger mass loss over 60% than the other two samples (the 0-Ni/CS precursor and the 4-Ni/CS precursor). The TG results further verified that an annealing temperature of 700 °C was suitable to obtain the targeted Ni/C electrocatalysts.

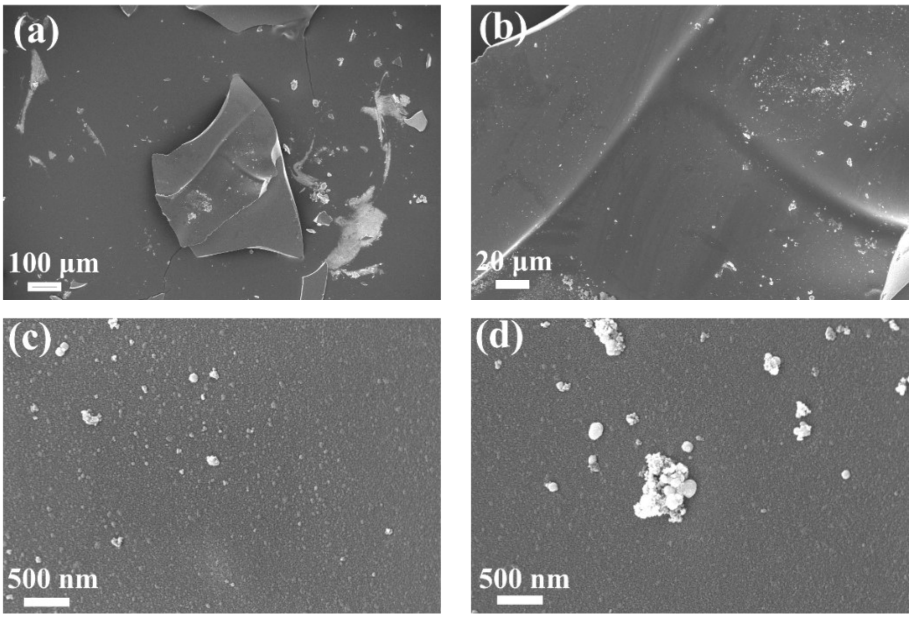

Fig. S7 SEM images of 4-Ni/CS-without NaCl sample at different magnitudes.

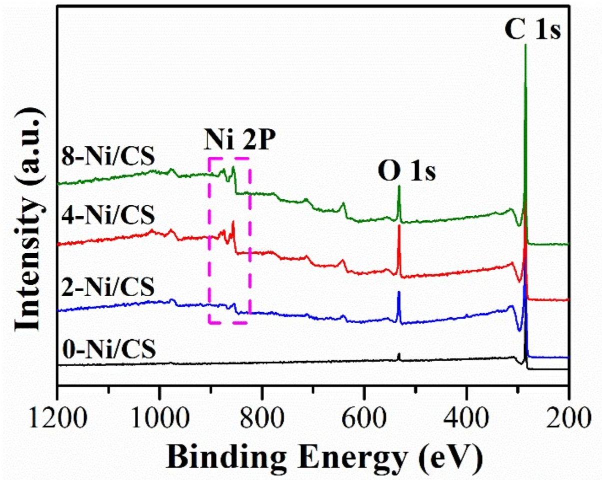

Fig. S8 XPS survey spectra of all x-Ni/CS samples.

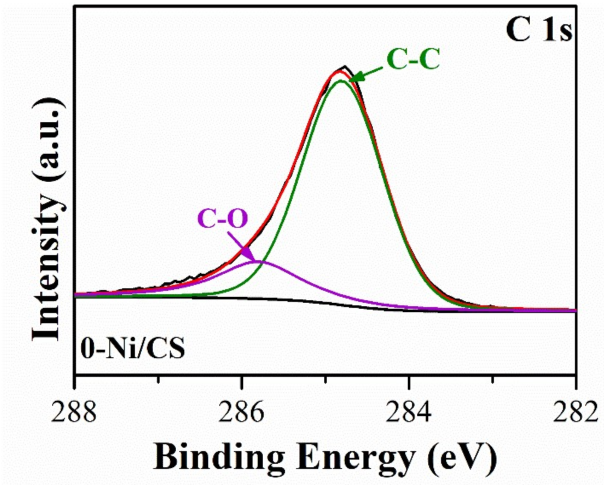

Fig. S9 High-resolution C 1s of 0-Ni/CS sample.

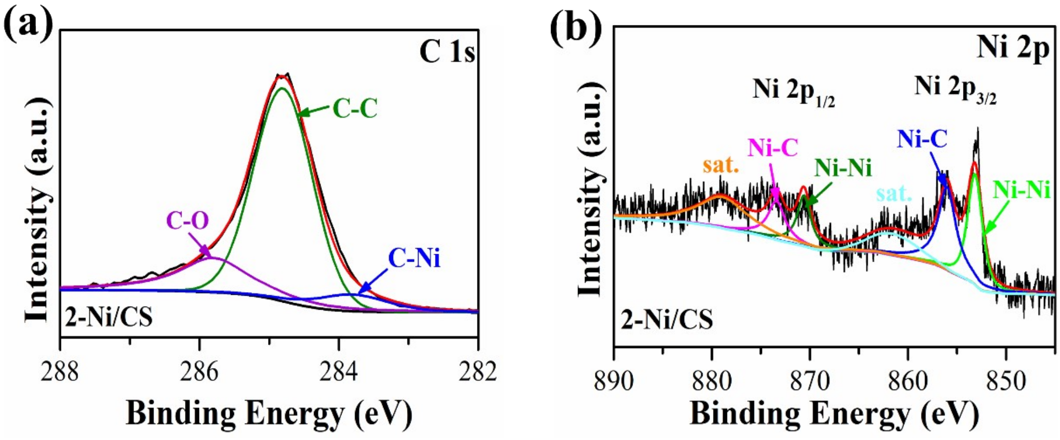

Fig. S10 High-resolution C 1s (a) and Ni 2p (b) of 2-Ni/CS sample.

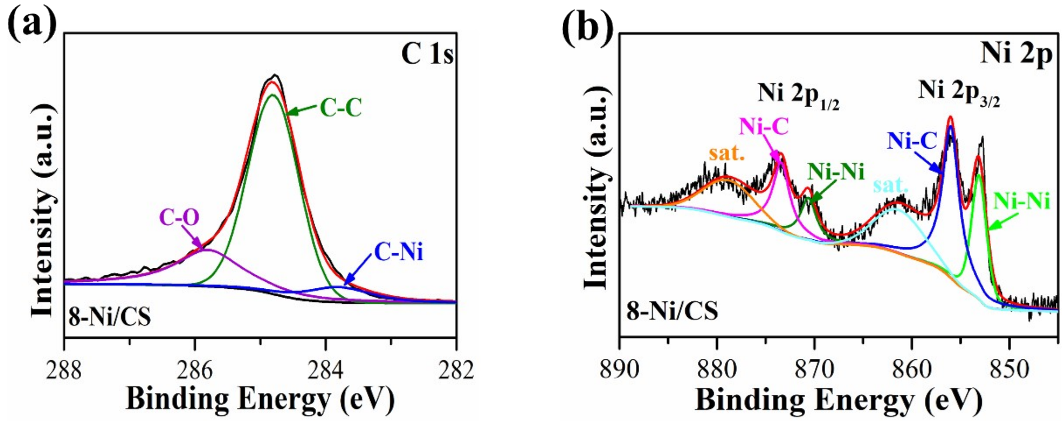

Fig. S11 High-resolution C 1s (a) and Ni 2p (b) of 8-Ni/CS sample.

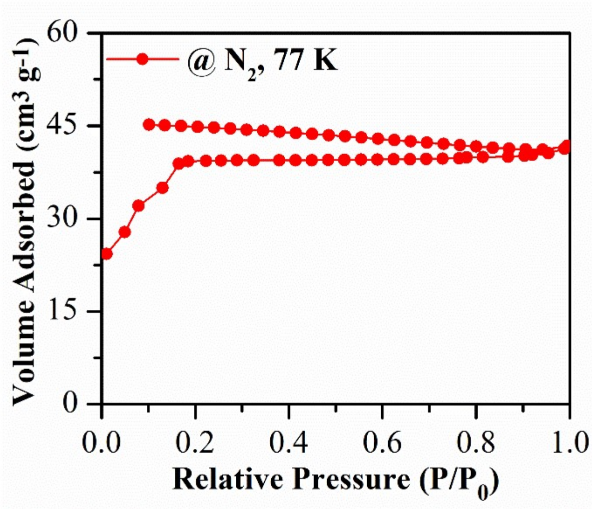

Fig. S12 N_2 sorption isotherm of 0-Ni/CS obtained from Micromeritics 3Flex.

Table S1 Textural and structural properties of 0-Ni/CS obtained from N_2 sorption experiment at 77 K.

Sample	**Analysis conditions**	**S_{BET} (m^2 g^{-1})**
0-Ni/CS	N_2, 77 K	144

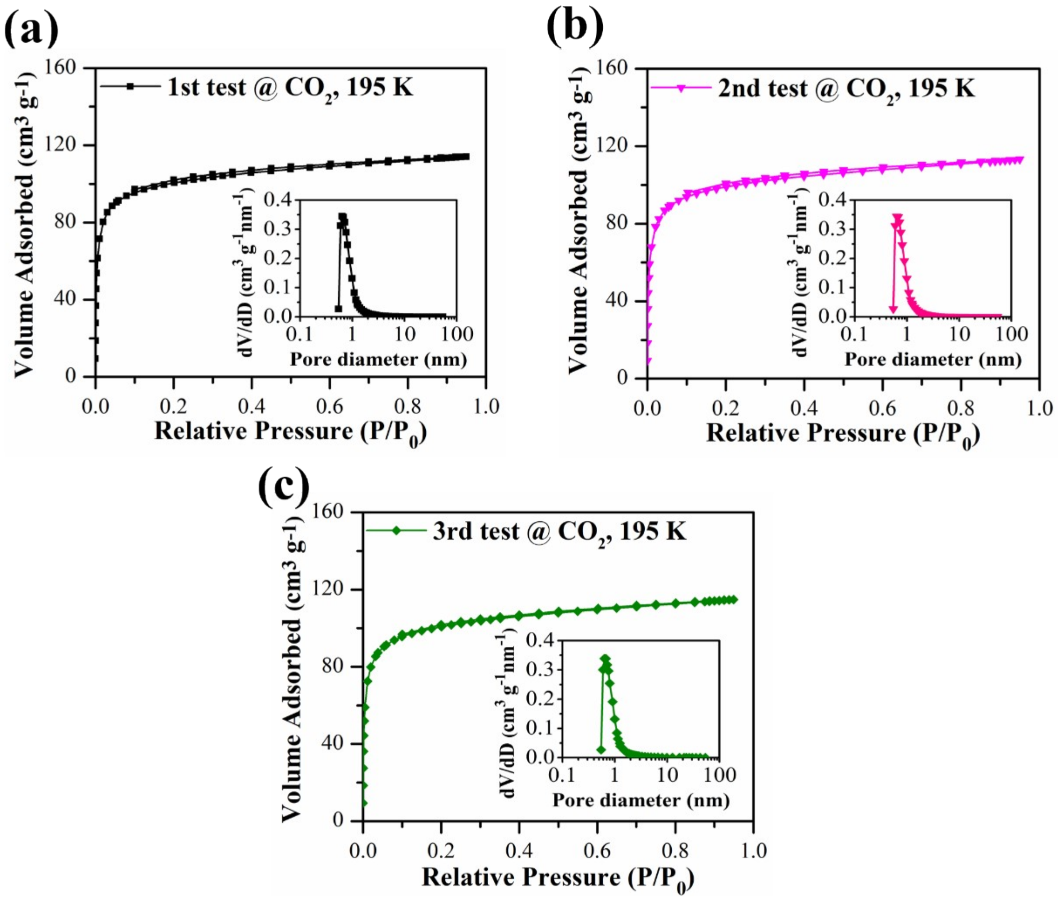

Fig. S13 CO_2 sorption isotherms and pore size distributions of 0-Ni/CS obtained from Micromeritics 3Flex for different times.

Table S2 Textural and structural properties of 0-Ni/CS obtained from CO_2 sorption experiments at 195 K.

Sample	**Analysis conditions**	**No.**	**Sample mass (mg)**	S_L [a] ($m^2\ g^{-1}$)	S_{BET} [b] ($m^2\ g^{-1}$)	V_p ($cm^3\ g^{-1}$)	D_p [c] (nm)
0-Ni/CS	CO_2,	1st	0.0958	382	342	0.18	0.78
	195 K	2nd	0.0741	376	338	0.18	0.80
		3rd	0.0595	383	344	0.18	0.79
Average value				380	341	0.18	0.79

[a] represents the Langmuir surface area

[b] represents the BET surface area

[c] estimated by applying the Horvath-Kawazoe equation.

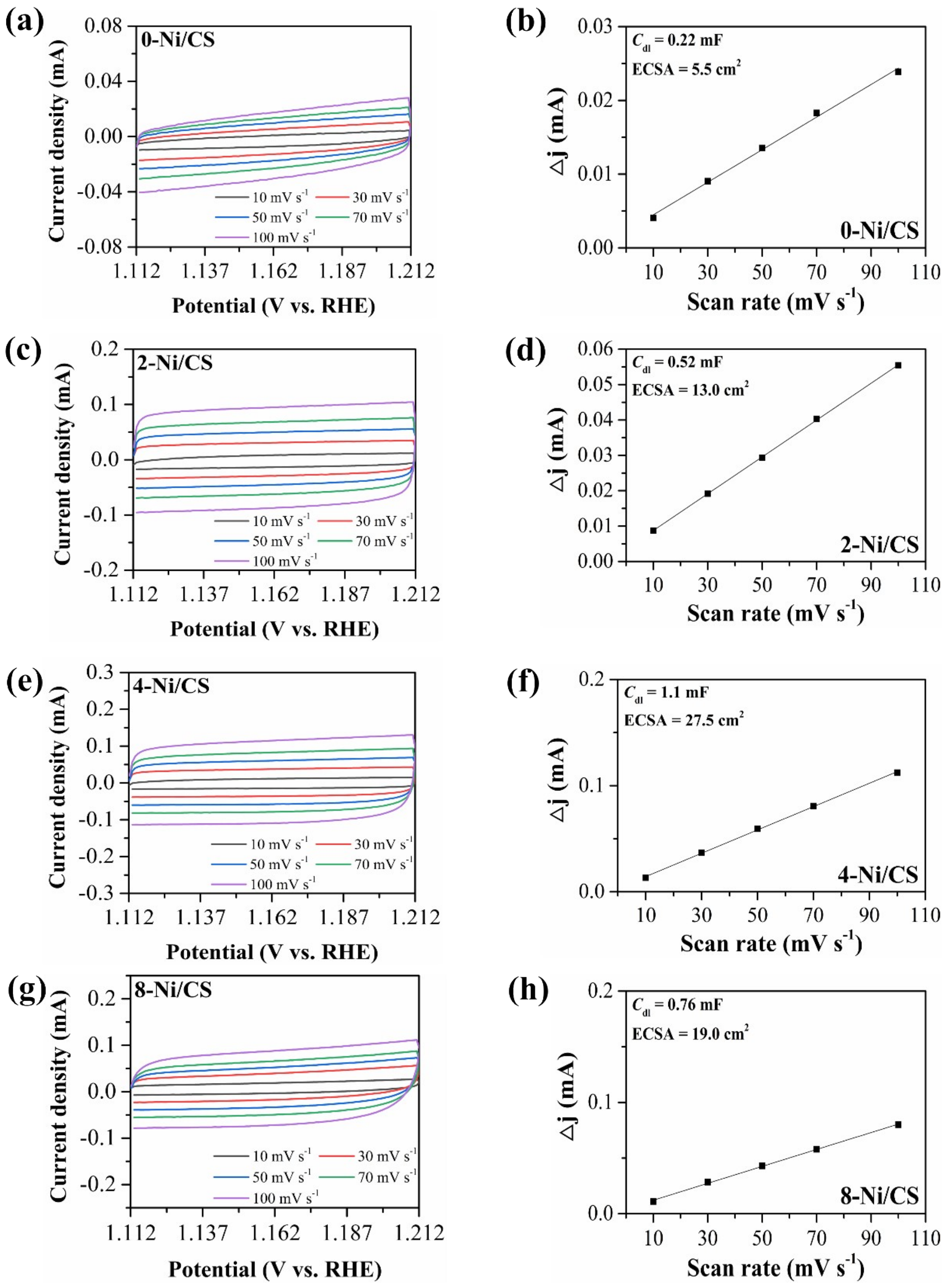

Fig. S14 CV curves of (a) 0-Ni/CS, (c) 2-Ni/CS, (e) 4-Ni/CS and (g) 8-Ni/CS in 1 M KOH and 0.33 M urea at different scan rates of 10, 30, 50, 70 and 100 mV s^{-1}; Current density recorded at 1.162 V vs. RHE as a function of scan rate for (b) 0-Ni/CS, (d) 2-Ni/CS, (f) 4-Ni/CS and (h) 8-Ni/CS.

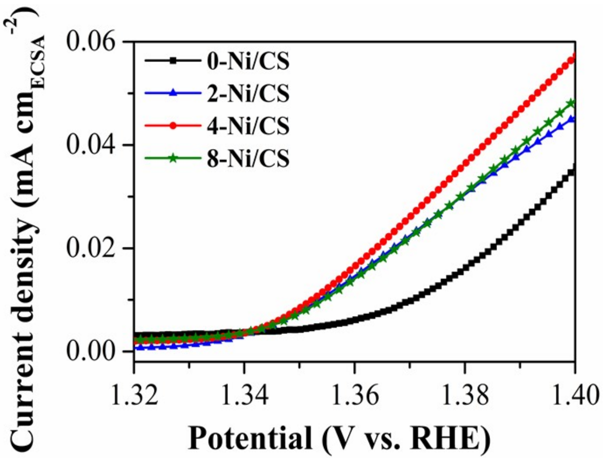

Fig. S15 *ECSA* normalized UOR LSV curves of x-Ni/CS samples in 1 M KOH and 0.33 M urea solution.

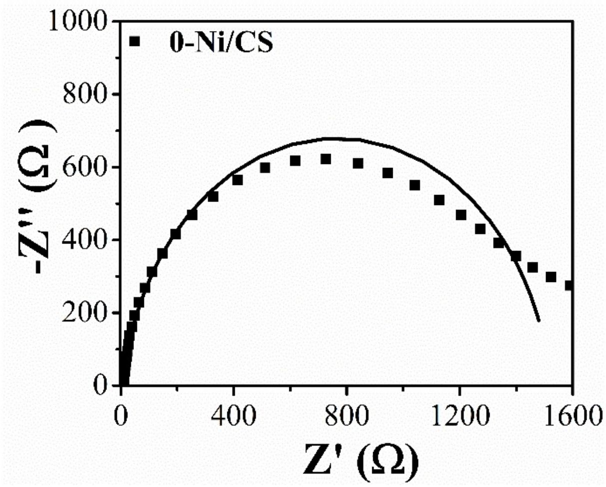

Fig. S16 Nyquist plots in 1 M KOH and 0.33 M urea for 0-Ni/CS.

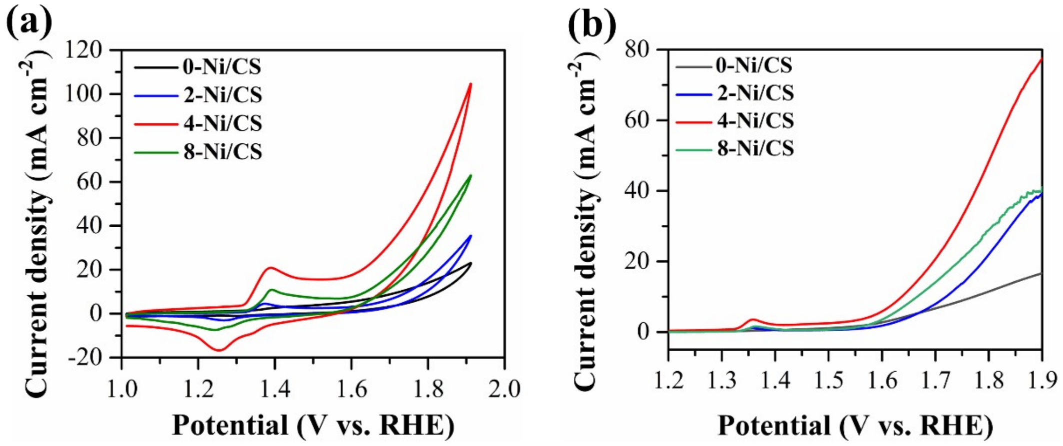

Fig. S17 CV curves (a) and LSV curves (b) in 1 M KOH for Ni/CS samples.

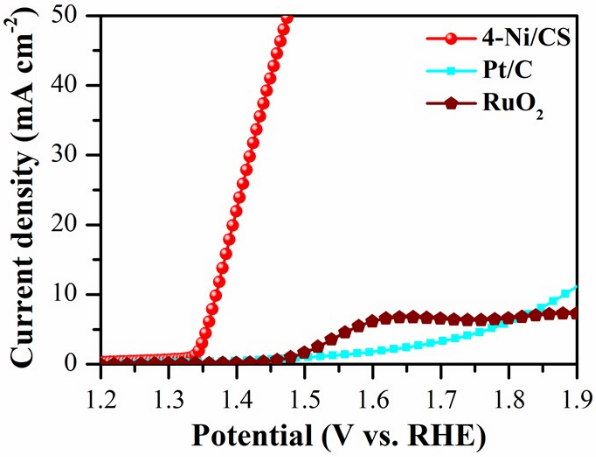

Fig. S18 The comparison of UOR LSV curves of 4-Ni/CS with the precious Pt/C or RuO_2.

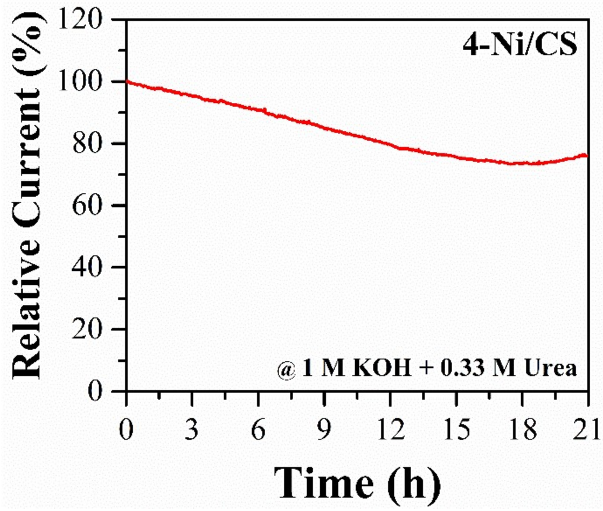

Fig. S19 Chronoamperometric responses of 4-Ni/CS in 1 M KOH and 0.33 M urea at a constant current density of 10 mA cm^{-2} for 21 h.

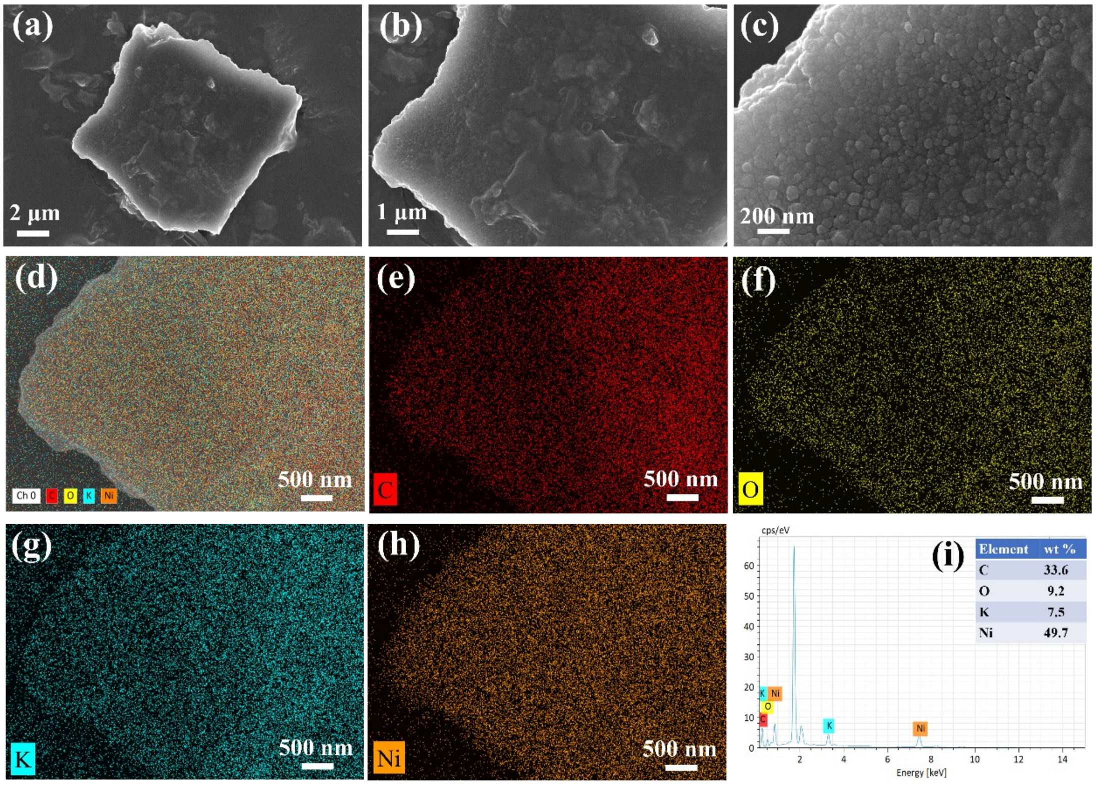

Fig. S20 SEM images (a-c), element mapping of (d) mix, (e) C, (f) O, (g) K and (h) Ni, and (i) SEM-EDS spectrum of the used 4-Ni/CS after the stability test for UOR.

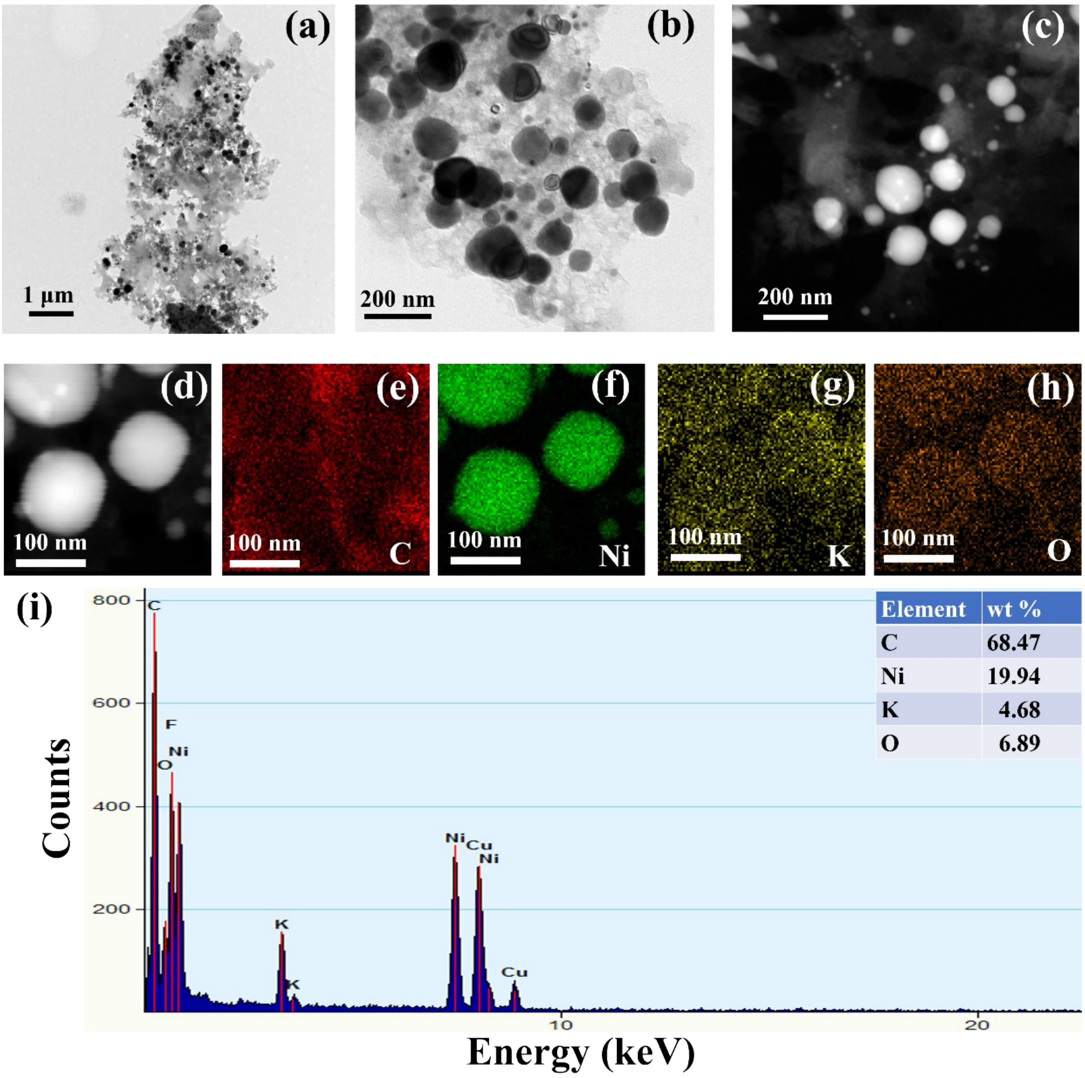

Fig. S21 TEM images (a-b), STEM-HAADF images (c-d), Element mapping of (e) C, (f) Ni, (g) K and (h) O, and (i) TEM-EDX spectrum of the used 4-Ni/CS after the stability test for UOR.

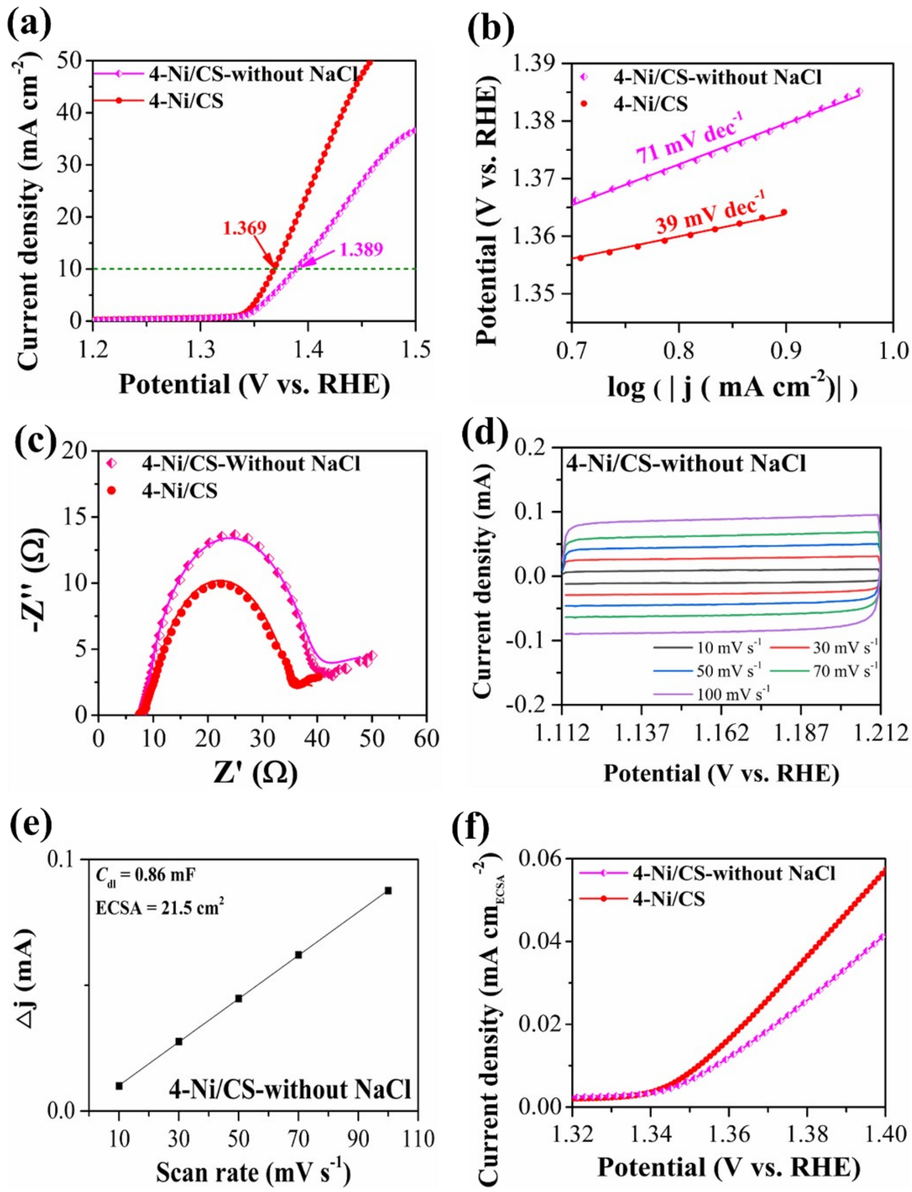

Fig. S22 (a) UOR LSV curves of 4-Ni/CS and 4-Ni/CS-without NaCl samples at a scan rate of 5 mV s^{-1} in 1 M KOH and 0.33 M urea; (b) the corresponding Tafel slopes for UOR; (c) Nyquist plots, (d) CV curves at different scan rates of 10, 30, 50, 70 and 100 mV s^{-1}, (e) the corresponding C_{dl} and ECSA values, and (f) ECSA normalized UOR LSV curves in 1 M KOH and 0.33 M urea.

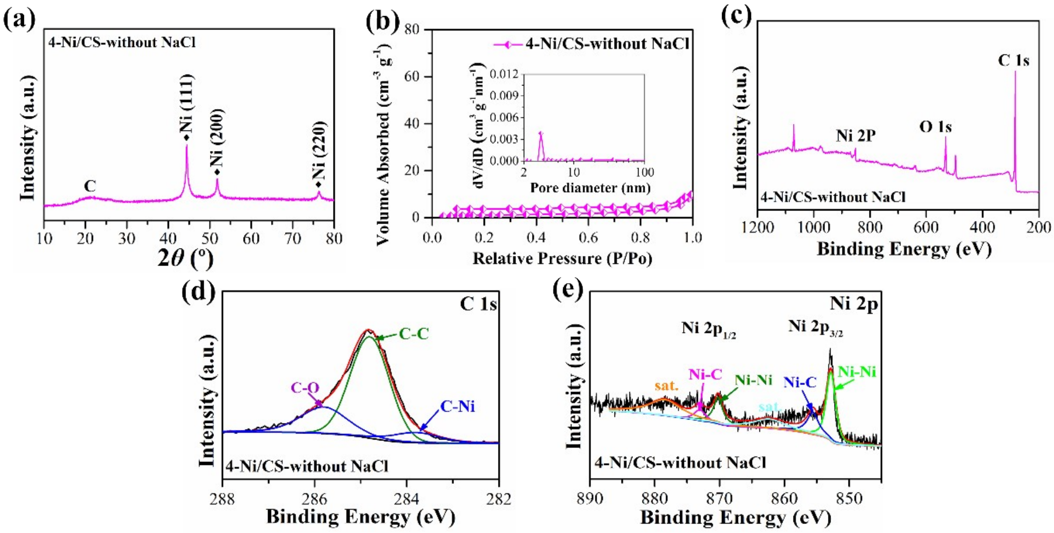

Fig. S23 XRD pattern (a), N_2 sorption isotherm and the inserted pore size distribution (b), XPS survey spectra (c), C 1s (d), and Ni 2p (e) of the 4-Ni/CS-without NaCl sample.

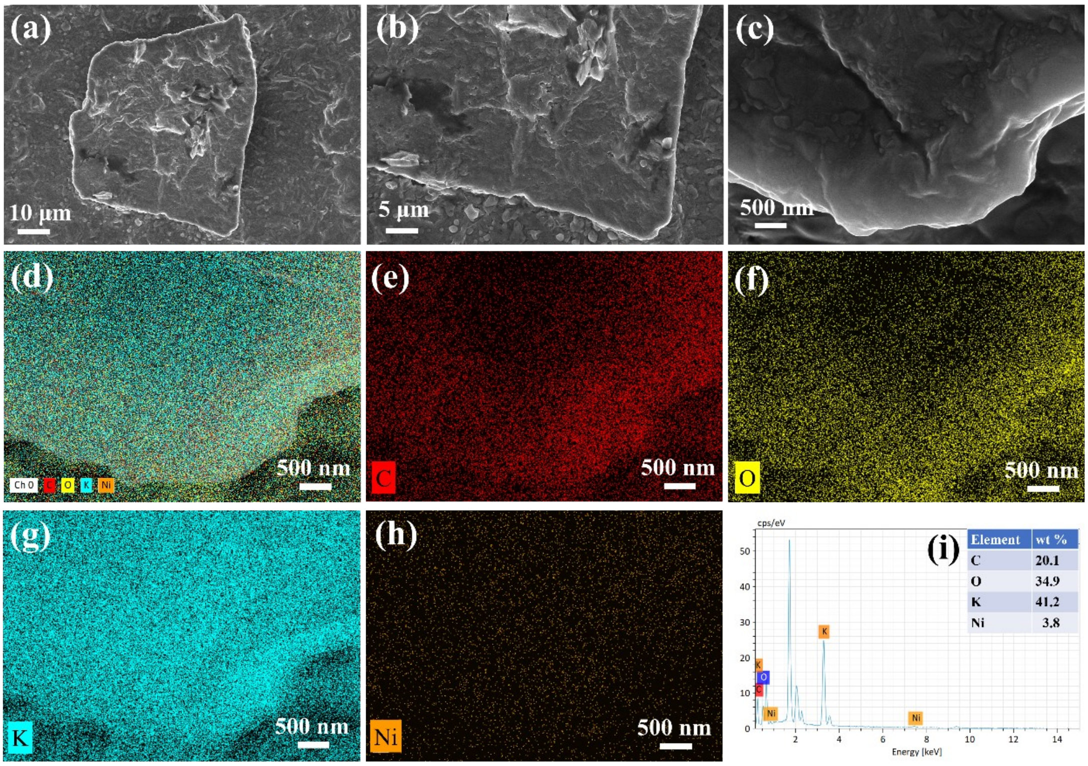

Fig. S24 SEM images (a-c), element mapping of (d) mix, (e) C, (f) O, (g) K, (h) Ni, and (i) SEM-EDX spectrum of the used 4-Ni/CS after the stability test for overall urea splitting.

Table S3 Textural and structural properties of 2-Ni/CS, 4-Ni/CS, 8-Ni/CS and 4-Ni/CS-without NaCl samples obtained from N_2 sorption experiments at 77 K.

Sample	**S_{BET} (m^2 g^{-1})**	**V_p (cm^3 g^{-1})**	**D_p (nm)**
2-Ni/CS	186	0.54	22.5
4-Ni/CS	128	0.39	23.5
8-Ni/CS	112	0.28	24.1
4-Ni/CS-without NaCl	0.8	0.002	-

a

Table S4 Ni content (wt%) in various samples by ICP-AES analysis.

Sample	**Ni content (wt%)**
0-Ni/CS	0
2-Ni/CS	46.3
4-Ni/CS	54.6
8-Ni/CS	64.5
4-Ni/CS-without NaCl	35.6

Table S5 Summary of the UOR and OER performances of Ni/CS samples.

Sample	**$UOR_{j=10}$ (V vs. RHE)**	**Tafel slope for UOR (mV dec^{-1})**	**$OER_{j=10}$ (V vs. RHE)**	**ΔE[a] (mV)**
0-Ni/CS	-	132	1.772	-
2-Ni/CS	1.412	109	1.720	308
4-Ni/CS	1.369	39	1.637	268
8-Ni/CS	1.387	71	1.666	279

[a] $\Delta E = OER_{j=10} - UOR_{j=10}$

Table S6 The simulated values of the devices in equivalent circuits.

Sample	R_s (Ω)	R_1 (Ω)	R_2 (Ω)	R_t (Ω)
0-Ni/CS	6.795	1512	2.08	1514.08
2-Ni/CS	7.986	78.45	35.32	113.77
4-Ni/CS	6.989	20.88	22.74	43.62
8-Ni/CS	7.084	25.24	26.67	51.91

Table S7 Comparison of the UOR performances of 4-Ni/CS with other reported Ni-based UOR catalysts in 1 M KOH and 0.33 M urea.

Sample	**Scan rate (mV s^{-1})**	**Potential @ 10 mA cm^{-2} (V vs. RHE)**	**Tafel slope (mV dec^{-1})**	**Ref.**
4-Ni/CS	**5**	**1.369**	**39**	**This work**
Ni-W_xC/CNTs	10	~1.37	-	1
Ni/NiO@NC	5	1.35	19	2
M-$Ni(OH)_2$	50	1.40	-	3
$Ni(OH)_2$ nanoflakes	20	1.37	36	4
$NiSe_2$-NiO	5	1.33	38	5
P-NTS-0.5	5	1.36	34	6
Ni-MOF@NiO/Ni-2	5	1.40	48.1	7
NixCo_{2-x}P/C@HCNs	5	1.33	74.6	8
$Ni(OH)_2$-graphene	10	1.43	-	9
Ni-MOF	10	1.36	23	10
Ni/C	10	1.38	77	11
35-NiS/NOMC	10	1.34	162.23	12
NiClO-D	5	1.341	41	13
NiOH-D	5	1.382	74	13
NiCo-2	10	1.38	51.1	14
NiCo-LDH-NO_3	-	1.32	91	15
CeO_2-$NiMoO_4$	10	1.35	35	16
NF/NiMoO-Ar	2	1.37	19	17
NiF_3/Ni_2P@CC	5	1.36	33	18
Fe-Ni_3S_2@$FeNi_3$-8	5	1.40	69	19

Table S8 Comparison of the performances of urea electrolyzer using 4-Ni/CS as the anode catalyst with other reported electrolysers.

Sample	Electrolyzer	Potential @ (mA cm^{-2})	Voltage (V)	Ref.
Pt/C@NF||4-Ni/CS@NF	**Urea electrolysis**	**10**	**1.372**	**This work**
	Water electrolysis	**10**	**1.572**	
Pt/C@NF||RuO_2@NF	**Urea electrolysis**	**10**	**1.388**	**This work**
NF||NF	**Urea electrolysis**	**10**	**1.702**	**This work**
Ni-W_xC/CNT||W_xC/CNTs	Urea electrolysis	10	1.65	1
P-NTS-0.5	Urea electrolysis	10	1.69	6
NixCo_2-xP/C@HCNs/CC	Urea electrolysis	10	1.47	8
NiCoFe-LTH/NF	Urea electrolysis	10	1.49	20
Pt/C||NiCo-2	Urea electrolysis	10	1.38	14
$NiCo_2S_4$ NS/CC	Urea electrolysis	10	1.45	21
CoFeCr LDH/NF	Urea electrolysis	10	1.329	22
NiFeRh-LDH/NF	Urea electrolysis	10	1.344	23
NF/NiMoO-Ar||NF/NiMoO-H_2	Urea electrolysis	10	1.38	17
NiF_3/Ni_2P@CC||NiF_3/Ni_2P@CC	Urea electrolysis	10	1.54	18
Fe-Ni_3S_2@$FeNi_3$-8||Fe-Ni_3S_2@$FeNi_3$-8	Urea electrolysis	10	1.50	19
MoS_2/Ni_3S_2/Ni/NF||MoS_2/Ni_3S_2/Ni/NF	Urea electrolysis	10	1.38	24

References

1. J. H. Fan, Y. P. Dou, R. Jiang, K. F. Du, B. W. Deng and D. H. Wang, *Int. J. Hydrogen Energy*, 2021, **46**, 14932-14943.
2. X. Y. Ji, Y. X. Zhang, Z. Ma and Y. F. Qiu, *ChemSusChem*, 2020, **13**, 5004-5014.
3. X. J. Zhu, X. Y. Dou, J. Dai, X. D. An, Y. Q. Guo, L. D. Zhang, S. Tao, J. Y. Zhao, W. S. Chu, X. C. Zeng, C. Z. Wu and Y. Xie, *Angew. Chem. Int. Ed.*, 2016, **55**, 12465-12469.
4. W. Yang, X. Yang, C. Hou, B. Li, H. Gao, J. Lin and X. Luo, *Appl. Catal. B-Environ.*, 2019, **259**, 118020.
5. Z. Liu, C. Zhang, H. Liu and L. Feng, *Appl. Catal. B-Environ.*, 2020, **276**, 119165.
6. Z. Ji, J. Liu, Y. Deng, S. Zhang, Z. Zhang, P. Du, Y. Zhao and X. Lu, *J. Mater. Chem. A*, 2020, **8**, 14680-14689.
7. Q. Li, S. Zheng, M. Du and H. Pang, *Chem. Eng. J.*, 2021, **417**, 129201.
8. S. Rezaee and S. Shahrokhian, *Nanoscale*, 2020, **12**, 16123-16135.
9. D. Wang, W. Yan, S. H. Vijapur and G. G. Botte, *Electrochim. Acta*, 2013, **89**, 732-736.
10. D. Zhu, C. Guo, J. Liu, L. Wang, Y. Du and S.-Z. Qiao, *Chem. Commun.*, 2017, **53**, 10906-10909.
11. L. Wang, L. Ren, X. Wang, X. Feng, J. Zhou and B. Wang, *ACS Appl. Mater. Interfaces*, 2018, **10**, 4750-4756.
12. R. Banerjee, D. Ghosh, Kirti, D. K. Chanda, A. Mondal, D. N. Srivastava and P. Biswas, *Electrochim. Acta*, 2022, **408**.
13. L. S. Zhang, L. P. Wang, H. P. Lin, Y. X. Liu, J. Y. Ye, Y. Z. Wen, A. Chen, L. Wang, F. L. Ni, Z. Y. Zhou, S. G. Sun, Y. Y. Li, B. Zhang and H. S. Peng, *Angew. Chem. Int. Ed.*, 2019, **58**, 16820-16825.
14. S. L. Wang, X. D. Yang, Z. Liu, D. W. Yang and L. G. Feng, *Nanoscale*, 2020, **12**, 10827-10833.
15. M. Zeng, J. H. Wu, Z. Y. Li, H. H. Wu, J. L. Wang, H. L. Wang, L. He and X. J. Yang, *ACS Sustain. Chem. Eng.*, 2019, **7**, 4777-4783.

16. W. Gao, C. Wang, F. Ma and D. Wen, *Electrochim. Acta*, 2019, **320**, 134608.
17. Z. Y. Yu, C. C. Lang, M. R. Gao, Y. Chen, Q. Q. Fu, Y. Duan and S. H. Yu, *Energy Environ. Sci.*, 2018, **11**, 1890-1897.
18. K. Wang, W. Huang, Q. Cao, Y. Zhao, X. Sun, R. Ding, W. Lin, E. Liu and P. Gao, *Chem. Eng. J.*, 2022, **427**, 130865.
19. W. Zhang, Q. Jia, H. Liang, L. Cui, D. Wei and J. Liu, *Chem. Eng. J.*, 2020, **396**, 125315.
20. K. Patil, P. Babar, H. Bae, E. Jo, J. S. Jang, P. Bhoite, S. Kolekar and J. H. Kim, *Sustainable Energy Fuels*, 2022, **6**, 474-483.
21. W. X. Zhu, M. R. Ren, N. Hu, W. T. Zhang, Z. T. Luo, R. Wang, J. Wang, L. J. Huang, Y. R. Suo and J. L. Wang, *ACS Sustain. Chem. Eng.*, 2018, **6**, 5011-5020.
22. Z. L. Wang, W. J. Liu, Y. M. Hu, M. L. Guan, L. Xu, H. P. Li, J. Bao and H. M. Li, *Appl. Catal. B-Environ.*, 2020, **272**.
23. H. C. A. Sun, W. Zhang, J. G. Li, Z. S. Li, X. Ao, K. H. Xue, K. K. Ostrikov, J. Tang and C. D. Wang, *Appl. Catal. B-Environ.*, 2021, **284**.
24. F. Li, J. Chen, D. Zhang, W.-F. Fu, Y. Chen, Z. Wen and X.-J. Lv, *Chem. Commun.*, 2018, **54**, 5181-5184.